

Northumbria Research Link

Citation: Rajbhandari, Sujan, Ghassemlooy, Zabih and Angelova, Maia (2009) Bit error performance of diffuse indoor optical wireless channel pulse position modulation system employing artificial neural networks for channel equalisation. IET Optoelectronics, 3 (4). pp. 169-179. ISSN 1751-8768

Published by: IET

URL: <http://dx.doi.org/10.1049/iet-opt.2007.0081> <<http://dx.doi.org/10.1049/iet-opt.2007.0081>>

This version was downloaded from Northumbria Research Link:
<http://nrl.northumbria.ac.uk/id/eprint/3241/>

Northumbria University has developed Northumbria Research Link (NRL) to enable users to access the University's research output. Copyright © and moral rights for items on NRL are retained by the individual author(s) and/or other copyright owners. Single copies of full items can be reproduced, displayed or performed, and given to third parties in any format or medium for personal research or study, educational, or not-for-profit purposes without prior permission or charge, provided the authors, title and full bibliographic details are given, as well as a hyperlink and/or URL to the original metadata page. The content must not be changed in any way. Full items must not be sold commercially in any format or medium without formal permission of the copyright holder. The full policy is available online: <http://nrl.northumbria.ac.uk/policies.html>

This document may differ from the final, published version of the research and has been made available online in accordance with publisher policies. To read and/or cite from the published version of the research, please visit the publisher's website (a subscription may be required.)

The Bit Error Performance of Diffuse Indoor Optical Wireless Channel PPM System Employing Artificial Neural Networks for Channel Equalization

S. Rajbhandari¹, Student MIET, Z. Ghassemlooy¹, FIT and M. Angelova²

¹Optical Communications Research Group

²Intelligent Modelling Lab

School of Computing, Engineering and Information Sciences, Northumbria University,
Newcastle upon Tyne, UK

Abstract

The bit error rate (BER) performance of a pulse position modulation (PPM) scheme for non line-of-sight (LOS) indoor optical links employing channel equalization based on the artificial neural network (ANN) is reported in the paper. Channel equalization is achieved by training a multilayer perceptrons (MLP) ANN. A comparative study of the unequalized ‘soft’ decision decoding and the ‘hard’ decision decoding along with the neural equalized ‘soft’ decision decoding is presented for different bit resolutions for optical channels with different delay spread. We show that the unequalized ‘hard’ decision decoding performs the worst for all values of normalized delayed spread becoming impractical beyond normalized delayed spread of 0.6. However, ‘soft’ decision decoding with/without equalization displays relatively improved performance for all values of the delay spread. The study shows that for a highly diffuse channel the signal-to-noise ratio (SNR) requirement to achieve a BER of 10^{-5} for the ANN based equalizer is ~ 10 dB lower compared with the unequalized ‘soft’ decoding for 16-PPM at a data rate of 155 Mbps. Our results indicate that for all range of delay spread, neural network equalization is an effective tool of mitigating the ISI.

1. Introduction

With current communication systems the bandwidth per end-user is limited at most to a few Mbps, because of the bottleneck imposed by the use of copper cables or radio frequency (RF) wireless links at the last mile. Although, higher RF frequencies (beyond 60 GHz) have been suggested to overcome the bandwidth bottleneck per user, the cost is too high and therefore may not be adopted by many users [1, 2]. Dropping fibre cable to homes is one solution, but is costly. One alternative solution would be to offer wireless links in the optical domain that could readily be linked to the high-speed optical fibre backbone link. Optical wireless (OW) systems (indoor and outdoor) offer all the advantages of optical fibre based systems plus rapid installation at a low cost and localised radiation resulting in no interference in adjacent cells/rooms. Compared with the RF based systems, OW offers a huge unregulated bandwidth at a single wavelength without resorting to the frequency reuse [1, 3, 4]. In fact the same wavelength could be used in a number of cells in the same geographical area with very little or no inter-channel interference. The cell size could be precisely defined in any shape for particular applications, a unique characteristic in OW systems.

However, in contrast to the RF system, OW links lacks mobility, blocking, eye and skin safety, ease of connectivity and suffers (only the non-line of sight (LOS)) from multipath induced inter-symbol-interference (ISI) similar to the RF links. Eye and skin safety could be improved by (i) operating at a higher wavelength of 1550 nm, where the laser beams are absorbed by the cornea and lens and do not focus on the retina [5], which is also compatible with third transmission window of the back-bone fibre optic links, and (ii) employing more power efficient modulation techniques. LOS link is the most power and bandwidth efficient since the optical power is highly concentrated and there is no loss or pulse dispersion due to multipath [6]. However, a LOS link requires precise alignment and suffers from blocking related link loss, thus limiting its application to a specific environment where there is no blocking at all. The coverage area in LOS links can be increased by broadening the transmitted beam to support mobility at the expense of power efficiency as in [7, 8], or by using non-LOS links.

Blocking can be mitigated to an extent at the cost of increased system complexity by employing a cellular concept [9]. Diversity techniques adopted at both the receiver and transmitter have also been used to reduce or eliminate the link loss due to blocking [10]. Blocking probability can also be reduced by adopting multiple inputs multiple outputs (MIMO)

systems, or a power efficient solution known as the data transmission with cycle emission, where light is emitted at different time slot in a cyclic fashion [8]. Mobility could be improved by utilizing a wide beam angle optical transmitter. In non-LOS links with no requirement for alignment, the existence of multipath links between the transmitter and the receiver eliminates the shadowing effect and blocking probability, but at the cost of increased path loss, reduced bandwidth and increased ISI compared with the LOS links [6, 9, 11, 12].

Although in OW systems the combination of intensity modulation and direct detection (IM/DD) prevents multipath fading, ISI still constitutes a major system impairment especially at high bit rates in an indoor environment [12-14]. In dispersive environment, the maximum likelihood sequence detection (MLSD) technique has been shown to give the optimum result; however, its complexity and delay prohibit its use in many applications [15]. A number of sub-optimum equalization techniques have been developed to combat the effect of ISI. In [16-18] equalization schemes for OW indoor links employing on-off-keying (OOK), PPM, and digital pulse interval modulation (DPIM) have been reported. The equalizers incorporated are mostly based on the digital finite impulse response (FIR) filters. Such equalizers are classified as a linear equalizer (without feedback) and a decision-feedback equalizer (DFE). In [17] it has been shown that a symbol rate zero-forcing DFE (ZF-DFE) outperforms a chip-rate ZF-DFE. This is because a complete PPM symbol, rather than a few slots, is being used as the feedback signal.

The adaptive equalization is a preferred method in a non-stationary environment. The equalizer attains the channel parameters in a supervised manner and adjusts its parameter based on the desired response within a given environment. In the traditional approach using the FIR filters, the filter coefficients are adjusted by transmitting a training sequence. The rationale behind using FIR filters is that by making the impulse response equal to the inverse of the channel, the filter will nullify the adverse effect of the channel at the receiver. More recently the equalization problem has been defined as a classification problem and ANN has been utilized as a classification tool [19-22]. In fact, both the linear and adoptive (using DFE) equalizers belong to a class of ANNs [23]. However, the classification capability of a linear equalizer is limited to a hyperplane decision boundary, which is a non-optimum classification strategy especially with respect to the time varying channel [24]. The optimum strategy would be to have a hyper-surface boundary for the classification. ANN with multiple layers of neurons is one of the best tools for implementing such a strategy. On the other hand adaptive processing,

universal approximation and self-organizing capabilities as well as adoptability to a non-Gaussian channel have made the ANN an appropriate tool for non-linear signal processing [25]. In fact, realization of an inverse filter is a more complex task than the pattern classification [23]. It has been reported that the adaptive DFE based on the ANN offers significantly superior BER performance compared to the conventional DFE for a severe amplitude distorted co-channel system [26] and non-linear channels [27].

Both the multilayer perceptrons (MLP) as well as the radial basic function (RBF) have been utilized for equalization [19, 20, 23, 27-29]. In comparison with the MLP, RBF requires a larger number of hidden nodes at lower values of SNR [29]. The cascaded MLP and RBF outperform both the MLP and RBF in terms of the BER performance [28]. ANN has been used in a number of communication fields including non-linear channel modelling, coding, decoding and error correcting codes, and non-linear signal processing to name a few [30].

To the best of our knowledge no work has been reported on the performance of the PPM system employing the neural equalization, which is the subject of this paper. Here, we have adopted ANN based ‘soft’ decision decoding to recover the original transmitted data. The paper is organised as follows: In Section 2 the PPM is introduced as a block code and algorithm for ‘soft’ decoding is presented. In Section 3, the ANN is introduced as an alternative adaptive equalizer to the FIR filter followed by description of the ANN based equalization scheme for PPM with a ‘soft’ decision decoding. Finally the simulation results for the BER performance are given in Section 5 and conclusions are presented in the Section 6.

2. PPM as a Block Code

A PPM is a baseband modulation technique most commonly used in optical communications (fibre optics as well as free space optics) because of unparallel power efficiency compared to any other baseband modulation technique. In the PPM, each set of M -bit input word $m = (a_1, a_2, \dots, a_M) \in (0,1)^M$ is mapped to one of L -array PPM symbols, where $L = 2^M$. L -PPM symbol $X = (0, \dots, 0, 1, 0, \dots, 0) \in (0,1)^L$ contains a single pulse of one time slot duration $T_s = M/(LR_b)$ and $L-1$ empty slots, where R_b is the data bit rate. The position of the pulse is indicated by the binary representation of m . PPM with a duty cycle of M^{-1} and a peak-to-average power ratio of M achieves the best power efficiency but at the cost of increased

bandwidth requirement compared to other pulse modulation schemes. A PPM signal can be written as:

$$x(t) = LP \sum_{M=0}^{L-1} c_M p\left(t - \frac{MT_f}{L}\right), \quad x(t) \geq 0 \text{ and } \overline{x(t)} \leq \overline{P}, \quad (1)$$

where $\overline{P} = L^{-1} \sum_j \overline{x_j(t)}$ is the average transmitted optical power, T_f is the symbol period, $[c_0, c_1, \dots, c_{L-1}]$ is the PPM code word. For the same bit rate, PPM requires L/M more bandwidth and a lower average power by a factor of $(0.5LM)^{0.5}$ compared to the OOK.

Considering the optimum single detection scheme using a matched filter and a threshold level detector, the slot error rate P_{se} for the PPM system can be approximated to [31]:

$$P_{se} = Q\left(\sqrt{\frac{1}{2} LM \frac{R\overline{P}}{\sqrt{N_0 R_b}}}\right), \quad (2)$$

where R is the photodetector responsivity, and N_0 is the one-sided power spectral density and the error function, $Q(\omega) = \frac{1}{\sqrt{2\pi}} \int_{-\omega}^{\infty} e^{-t^2/2} dt$.

As each symbol contains L slots, the probability of symbol error is $P_{e-sym} = 1 - (1 - P_{se})^L$. If we consider all symbols to be equally likely, then the probability of symbol error may be converted into a corresponding bit-error rate by the following [15]:

$$P_{e-bit} = \frac{L}{2(L-1)} P_{e-sym}. \quad (3)$$

In the diffuse channel, it is not easy to approximate the error probability of equalized system. Instead, the upper bound and the lower bound are calculated by averaging the error probabilities by randomly chosen transmitted sequence [32].

In addition to the power efficiency, PPM symbols have built-in error detection capability. Since PPM can be considered as a block code with a Hamming distance of one, both the ‘hard’ decision decoding and the ‘soft’ decision decoding schemes can be applied. Although the later is computationally complex compared to the former, it offers SNR gain of more than 1.5 dB in a LOS link and higher gains in non-LOS Links [6]. In PPM employing a simple L -input comparator, ‘soft’ decision decoding is carried out by finding a correlated matrix with the highest average amplitude. Consider a block code with N possible combinations ($N = L$ for

PPM). Following the similar approach taken in [33] and taking into consideration that optical system has no negative energy, the received sequence r_j is given by:

$$\begin{aligned} r_j &= \sqrt{E} + n_j & \text{if } j^{\text{th}} \text{ bit is 1} \\ r_j &= n_j & \text{if } j^{\text{th}} \text{ bit is 0} \end{aligned}, \quad (4)$$

where n_j represents the zero mean white Gaussian noise, and E is the energy per bit and $j = 1, \dots, N$. The decoding aims to find N dimensional vector with elements given by:

$$CM_i = \sum_{j=1}^N c_{ij} r_j, \quad (5)$$

where c_{ij} denotes the bit in the j^{th} position of the i^{th} code word and $i = \{1, \dots, N\}$. Hence $c_{ij} = \{0, 1\}$ depending upon the bit corresponding to 0 and 1 respectively. Since a PPM symbol contains only one pulse, the value of CM_i depends only on the non-zero bit of the i^{th} code word. Hence the ‘soft’ decoding can be carried out by assigning “1” to the bit with highest amplitude and “0” to the remaining bits. To clarify the concept, consider 4-PPM with received symbol $\mathbf{r} = \{r_1, r_2, r_3, r_4\}$. Then CM is given by:

$$CM = \begin{bmatrix} 1 & 0 & 0 & 0 \\ 0 & 1 & 0 & 0 \\ 0 & 0 & 1 & 0 \\ 0 & 0 & 0 & 1 \end{bmatrix} [r_1 \ r_2 \ r_3 \ r_4] = \begin{bmatrix} r_1 \\ r_2 \\ r_3 \\ r_4 \end{bmatrix} \quad (6)$$

Since the values $CM_i = r_j$ for $i = j$, selecting a codeword corresponding to the maximum value of CM_i is equivalent to assigning “1” to the bit with the highest amplitude.

3. Artificial Neural Network Adaptive Equalizer

Fundamentally, the problem of adaptive equalization can be formulated as a classification problem [24, 34], and modern classifying tools like ANN can be utilised. ANN is more suitable for channel equalization because of highly parallel structure, adaptability and learning capability. Since there is no need for channel inversion then ANN equalization can be implemented in any channel. The functional unit of ANN is a neuron. A neuron cannot perform a complicated task on its own, but when combined and interconnected in some predefined manner, the composed ANN create a powerful tool for difficult tasks including nonlinear signal processing, adaptive learning, solution of nonlinear equations to name a few. Haykin [25] has pointed out the rationale behind using ANNs instead of the traditional signal processing tools, the most importantly being the nonlinearity, universal approximation, adaptability to change its free parameter based on the environmental changes.

Figure 1 shows the block diagram of a single hidden layer feedforward ANN, where the output of a neuron is given by:

$$y = f\left(b + \sum_{k=1}^n x_k \cdot w_k\right), \quad (7)$$

where w_k is the weight associated with input x_k to the neuron, f is the activation function, and 'b' is the bias to the ANN. The bias can be considered as an input with a constant weight of one. The sigmoid function and the linear function are the common activation functions used in ANN for a classification purpose, though other activation functions like the linear and threshold functions are also used [35].

The MLP may have more than one hidden layer, Fig. 1(b). The neurons in each layer are connected to the every other neurons in adjust layers. The signal flows in feedforward manner, hence is called feedforward MLP. The activation function in the hidden layer can be sigmoid or linear. The two outer layers, which receive inputs from or provide outputs to the external environment are called the input layer and output layer, respectively according to their function. For equalization, ANN is trained in supervised manner by providing input-output sets and adjusting free parameters, the weights and the bias, to minimise the error between the actual output $y(n)$ and target output $d(n)$. There are different training algorithms, the most popular being the backpropagation (BP) learning in which the weights in n^{th} iteration are updates as:

$$w_{ij}(n + 1) = w_{ij}(n) - \eta \frac{\partial E(n)}{\partial w_{ij}(n)} ; \quad (8)$$

where $w_{ij}(n)$ is the weight from the hidden node i to the node j , η is the learning rate parameter and $E(n) = \|d(n) - y(n)\|^2$ is an error function. The target of training algorithm is to reduce the value of $E(n)$ for each iteration until it reaches a constant value.

The equalizer structure based on the ANN is shown in Fig. 2. Like traditional equalizers, the received signal $u(n)$ is passed through tap delay lines (TDL) of length L , where L depends on the channel delay spread. The free parameters (weight and bias) of the ANN are adjusted according to the channel condition by transmitting a training sequence. MLP as well as the radial basis function network and the recurrent ANN have been proposed and applied for

channel equalization, details of which can be found in [20, 23, 24, 34, 36] and references therein. This study is limited to the equalization using the feedforward MLP with BP training algorithm.

4. PPM System with AAN Equalization

The block diagram of neural equalized PPM is given in Fig. 3. M -bit binary data sequence $\{b_j\}$ passed through a serial-to-parallel converter is converted into an L -PPM sequence $\{x_j\}$. PPM symbols are then passed to a transmitter filter with a unit-amplitude rectangular impulse response $P(t)$ of one time slot duration T_s . The resulting continuous time signal $X(t)$ is transmitted through the optical channel with impulse response of $h(t)$. The noise signal $n(t)$ is modelled as the additive white Gaussian (AWGN) and it is independent of $X(t)$. The channel is assumed to be time invariant and the model for diffuse indoor optical wireless link adopted here is based on the well known Ceiling bounce model with an impulse response given by [37] :

$$h(t) = H(0) \frac{6a^6}{(1+a)^3} u(t), \quad (9)$$

where H is the height of the ceiling above the transmitter and receiver, c is the velocity of light and $u(t)$ is a unit step function. The parameter $a = 2H/c$ is related to the root mean square (rms) delay spread D_{rms} given by:

$$D_{rms}(h(t)) = \frac{a}{12} \sqrt{\frac{13}{11}}. \quad (10)$$

For a more realistic channel model with multiple reflections, “ a ” needs to be modified. For the unshadowed and the shadowed channels the expressions for a is given by [37]:

$$a(\text{unshad.}) = 12 \sqrt{\frac{11}{13}} (2.1 - 5.0s + 20.8s^2) D_{rms}(h_1(t)), \quad (11)$$

$$a(\text{shad.}) = 12 \sqrt{\frac{11}{13}} (2.0 + 9.4s) D_{rms}(h_1(t)), \quad (12)$$

where s is defined as the ratio of the horizontal transmitter-receiver separation to the TR diagonal, the latter is defined as the length of the segment of the line between the transmitter and the receiver.

The multipath channel is characterised by D_{rms} and the optical path loss $H(0)$, contributing to ISI and signal attenuation respectively. Here $H(0)$ is assumed to be negligible and is therefore normalized to unity. The delay spread contributing to the ISI is usually normalized to T_s given as:

$$D_T = D_{rms}/T_s. \quad (13)$$

The received optical signal $Z(t) = \sum_{n=1}^N \tilde{C}_n$, where $S(t) = X(t) \otimes h(t)$, is first converted to its electrical equivalent, which is then passed through the matched filter with impulse response $r(t) = P(-t)$ matched to the transmitted pulse. The discrete-time equivalent impulse response of the cascaded system truncated to have j time slots is given by:

$$C_j = P(t) \otimes h(t) \otimes r(t) \Big|_{t=jT_s}. \quad (14)$$

The output from the filter is sampled at the end of each slot at the slot rate, and the sampled output sequence u_j is applied to the ANN for classification (Fig. 3). The estimated PPM sequence $\{\hat{x}_j\}$ at the output of the ANN is passed through a serial-to-parallel converter prior to being applied to the ‘soft’ decision decoder to regenerate the PPM symbols. Finally, a PPM decoder will recover the input data binary sequence $\{\hat{b}_j\}$. In the case of the ‘hard’ decision decoding, a PPM symbol is generated by keeping the first pulse in the decoded PPM symbol and setting the rest to zero.

In this work, a feed-forward back propagation ANN with 36 neurons in the 1st layer and a single neuron in the 2nd layer is used. The transfer functions adopted for the 1st and 2nd layers are the tan-sigmoid and the log-sigmoid, respectively. To estimate the channel parameters, ANN is trained by transmitting a predefined 1.2 kbits binary data sequence at a regular interval. The scaled conjugate gradient algorithm [38] is adopted to adjust the ANN weights and biases. The learning duration and the number of iteration required to adjust the ANN parameters depend on the complexity of the learning task. Here the aim is not to optimize the learning task but to let the ANN to estimate the new channel parameters by sending a learning sequence of a certain length. Once the ANN is fully trained, the detection process of the received signal will commence.

A Monte Carlo simulation is carried out using 1000 PPM symbols per packet. The simulation is stopped if the number of erroneous bits received is at least 100 for $\text{BER} > 10^{-3}$. However, because of long computational time, the number of erroneous bits is limited to 10 for $\text{BER} < 10^{-3}$. In this work, we compare the input bit sequence b_j and output bits sequence \hat{b}_j to evaluate the error performance rather than the conventional way of comparing the input and output PPM symbol sequences. Hence, BER is used as the measure of performance evaluation.

5. Results and Discussion

Using the simulation parameters given in Table 1, the system performance is investigated. Equations (2) and (3) are used to plot the BER for the LOS link with ‘hard’ decision decoding. The simulated BER is obtained using the procedure shown in Fig. 4 using Matlab.

Figure 5 depicts the normalised discrete impulse responses of diffuse channel with and without equalization at $D_{rms} = 5$ ns. Note that the impulse response is normalised by dividing values in each sampling instant by $\sum_{j=0}^{\infty} h(t)|_{t=j\tau}$ where τ is the sampling instant and the channel delay is removed in the ceiling bounce model by shifting the time origin by $2H/c$. Though, pulse spreading depends only on the channel parameter, i.e. D_{rms} , whereas the ISI depends on both $h(t)$ and R_b . The impulse response of a cascaded system (i.e. convolved response of the channel and the ANN equalizer) as in Fig. 5(b) shows a response similar to the ideal case, where the ANN has effectively compensated for the channel impairments (pulse spreading). The high amplitude in the impulse response in Fig. 5(b) is due to normalization. Note, practically it is not possible to obtain an ideal response even with an equalizer because of numerous factors such as the channel noise and the time varying channel parameters. In [39] it has been shown that for the ceiling bounce channel model both the ANN and linear FIR digital filter equalizers display identical BER performance for the ‘hard’ decision decoding. Hence in this work we report only the performance comparison of the ‘hard’ decision decoding and the unequalized and ANN based equalizer with the ‘soft’ decision decoding.

Figure 6 illustrates the BER performance curves against the SNR for ANN equalized and unequalized 8-PPM for diffuse links employing ‘soft’ decision decoding scheme at a data rate of 155 Mbps for D_{rms} value of 1 and 5 ns. Also presented for comparisons are the simulated BER curves for the LOS link with ‘hard’ and ‘soft’ decision decoding and predicted results for ‘hard’ decoding using (2) and (3), showing a good agreement with the simulation. As reported

in [40, 41] and confirmed by our simulations the ambient light does not affect BER performance in LOS and dispersive channel with ‘soft’ decision decoding at high data rate of 155 Mbps. Thus, it is not taken into consideration. As can be seen at BER of 10^{-5} , LOS link with the ‘soft’ decision decoding displays the best performance offering a SNR gain of ~ 3 dB compared to the LOS with the ‘hard’ decoding. For the diffuse channel, the unequalized ‘hard’ decision decoding displays the least desirable performance. The unequalized ‘hard’ decision BER performance for a highly dispersive channel (i.e. $D_{rms} = 5$ ns) displays a higher error rate thus it is of no practical use. The ‘soft’ decision decoding with no equalization offers a much improved performance compared to the ‘hard’ decoding for LOS and diffuse cases. In ‘soft’ decoding, signals with the largest cross correlation between the received vector r and possible transmitted signal vector as in (5) is selected, thus providing the optimum performance in LOS links. In diffuse links with matched filter and threshold detection ISI induced noise is still a problem particularly at high values of D_T . Using an equalizer with ‘soft’ decoding capability (the optimum detection) reduced the effect of ISI, thus leading to improved performance. The ‘soft’ decision decoding scheme offer ~ 4.5 dB SNR gain at BER of 10^{-5} at D_{rms} of 1 ns compared to the ‘hard’ decision decoding. The gain increases for higher values of D_{rms} . Compared to LOS links (‘soft’ decoding), additional SNR of ~ 2 dB and ~ 15 dB are required to achieve a BER of 10^{-5} for a diffuse channel with D_{rms} of 1 ns and 5 ns, respectively without incorporating any equalizer. The BER performance of equalized case with ‘soft’ decoding displays a striking improvement compared to unequalized ‘hard’ and ‘soft’ cases. The performance gain using equalization increases as the channel becomes more dispersive. For example, for D_{rms} value of 5 ns, equalized ‘soft’ scheme requires ~ 8 dB low SNR than the unequalized ‘soft’ decoding to achieve the same BER of 10^{-5} .

Figure 7 illustrates the SNR required to achieve a BER of 10^{-5} at a data rate of 155 Mbps for a range of D_T from 0 to 4 for all three cases being investigated; unequalized ‘hard’ decoding, unequalized ‘soft’ decision decoding and equalization with ‘soft’ decision decoding for 4, 8 and 16-PPM . It is evident that BER performance of unequalized ‘hard’ decision decoding is very susceptible to D_T [42]. There is an exponential increment in the SNR requirement to achieve a BER of 10^{-5} with increase D_T . High values of SNR penalties (> 20 dB) are incurred for the $D_T > 0.5$, thus making the ‘hard’ decoding impractical for highly diffuse channel. Whereas the system employing the ‘soft’ decision decoding (equalized and unequalized) shows much more resistance to the channel spreading with the ANN equalized ‘soft’ decoding offering the best performance for all values of D_T . There is a linear increment in the SNR

requirement for both the unequalized and equalized ‘soft’ decoding schemes with the latter offering much improved SNR gain as channel gets more dispersive. Compared to the unequalized ‘hard’ decision decoding, the SNR requirement to achieve a BER of 10^{-5} for 16-PPM with the D_T of 0.6 is 9 and 10.5 dB lower for unequalized ‘soft’ and ANN equalized ‘soft’ decoding, respectively. At the normalized $D_{rms} > 0.6$ both SNR power penalties for the unequalized ‘soft’ and ANN equalized decoding are considerably lower compared with the unequalized ‘hard’ decoding. For example, at D_T of 3, the unequalized ‘hard’ decision decoding is no longer feasible as SNR requirement is impractical whereas ‘soft’ decision decoding without/with an equalizer requires only 18 and 10 dB higher SNR compared to the LOS case. This result shown clearly demonstrates the potential of ANN based equalizer with the ‘soft’ decoding for dispersive environment. As expected, higher SNR penalties are incurred for lower orders of PPM.

6. Conclusion

The paper has proposed ANN based equalizer with ‘soft’ decision decoding as an alternative tool to mitigate the multipath induced ISI equalization for indoor optical wireless links. The unequalized/equalized performance of ‘soft’ and ‘hard’ decision decoding for 4, 8 and 16-PPM for a range delay spread at the data rate of 155Mbps was evaluated using the Monte Carlo simulation. It was shown that the unequalized ‘hard’ decision decoding performed the worst for all values of normalized delayed spread becoming impractical beyond normalized delayed spread of 0.6. However, ‘soft’ decision decoding with/without equalization displayed relatively improved performance for all values of the delay spread. For a highly diffuse channel (i.e. normalized delay spread of 3) the SNR power penalty for the ANN based equalizer is 10 dB lower compared with the unequalized ‘soft’ decoding for 16-PPM at a data rate of 155 Mbps. The results show that for all range of delay spread, neural network equalization is an effective tool of mitigating the ISI. The practical implementation of the ANN based equalizer is the subject of further study.

Acknowledgement

One of the authors (Mr. S. Rajbhandari) is sponsored by the Northumbria University.

References

- [1] R. D. Wisely, "A 1 Gbit/s optical wireless tracked architecture for ATM delivery," in *IEE Colloquium on Optical Free Space Communication Links* London, UK, 1996.
- [2] D. A. Rockwell and G. S. Mecherle, "Optical wireless: low-cost, broadband, optical access," SONA Communications Corporation, 2007.
- [3] K. K. Wong, T. O'Farrell, and M. Kiatweerasakul, "The performance of optical wireless OOK, 2-PPM and spread spectrum under the effects of multipath dispersion and artificial light interference," *International Journal of Communication Systems*, vol. 13, pp. 551-57, 2000.
- [4] J. B. Carruthers and P. Kannan, "Iterative site-based modeling for wireless infrared channels," *IEEE Transactions on Antennas and Propagation*, vol. 50, pp. 759-765, 2002.
- [5] D. A. Rockwell and G. S. Mecherle, "Wavelength selection for optical wireless communications systems," *Proc. of SPIE*, vol. 4530, pp. 27-35, 2001.
- [6] J. M. Kahn and J. R. Barry, "Wireless infrared communications," *Proceedings of IEEE*, vol. 85, pp. 265-298, 1997.
- [7] A. G. Al-Ghamdi and J. M. H. Elmirghani, "Multiple spot diffusing geometries for indoor optical wireless communication systems," *International Journal of Communication Systems*, vol. 16, pp. 909-922, 2006.
- [8] H. Takano and S. Shimamoto, "A study of optical wireless mobile communications with movable cells employing cycle emissions," *Electronics and Communications in Japan (Part I: Communications)*, vol. 87, pp. 45-57, 2004.
- [9] A. M. Street, P. N. Stavrinou, D. C. Obrien, and D. J. Edwards, "Indoor optical wireless systems - A review," *Optical and Quantum Electronics*, vol. 29, pp. 349-378, 1997.
- [10] P. Djahani and J. M. Kahn, "Analysis of infrared wireless links employing multibeam transmitters and imaging diversity receivers," *IEEE Transactions on Communications*, vol. 48, pp. 2077-2088, Dec. 2000.
- [11] Z. Ghassemlooy, A. R. Hayes, and N. L. Seed, "The effect of multipath propagation on the performance of DPIM on diffuse Optical wireless communications," in *Proceedings of the IASTED International conference on wireless and optical communications* Canada, 2001, pp. 166-172.

- [12] Z. Ghassemlooy, A. R. Hayes, and B. Wilson, "Reducing the effects of intersymbol interference in diffuse DPIM optical wireless communications," *IEE Proceedings optoelectronics*, vol. 150, pp. 445 - 452, 2003.
- [13] H. Park and J. R. Barry, "Trellis-coded multiple pulse position modulation for wireless infrared communications," *IEEE Transactions on Communications*, vol. 54, pp. 643-651, 2004.
- [14] J. B. Carruthers and P. Kannan, "Iterative site-based modeling for wireless infrared channels," *IEEE Transactions on Antennas and Propagation*, vol. 50, pp. 759-765, May 2002.
- [15] J. G. Proakis, *Digital communications*, Fourth ed. New York: McGraw-Hill, Inc., 2001.
- [16] J. R. Barry, "Sequence detection and equalization for pulse-position modulation," *International Conference on Communication*, New Orleans, LA, 1994, pp. 1561-1565.
- [17] M. D. Audeh, J. M. Kahn, and J. R. Barry, "Decision-feedback equalization of pulse-position modulation on measured nondirected indoor infrared channels," *IEEE Transaction on Communications*, vol. 47, pp. 500-503, 1999.
- [18] A. R. Hayes, "Digital pulse interval modulation for indoor optical wireless communication systems," Sheffield Hallam University, UK, 2002.
- [19] J. Feng, C. K. Tse, and F. C. M. Lau, "A Neural-Network-Based Channel-Equalization Strategy for Chaos-Based Communication Systems," *IEEE Transaction on Circuits and Systems-I; Fundamental Theory and Applications*, vol. 50, pp. 954-957, 2003.
- [20] A. K. Tripathy and K. T. Raghavendra, "An efficient channel equalizer using artificial neural networks," *Proceeding of 4th International Multiconference on Computer Science and Computer Technology*, vol. 4, pp. 357-368, 2006.
- [21] D. Jianping, N. Sundararajan, and P. Saratchandran, "Communication channel equalization using complex-valued minimal radial basis function neural networks," *IEEE Transactions on Neural Networks*, vol. 13, pp. 687-696, May 2002.
- [22] W. Chagraa, F. Bouanib, R. B. Abdenourc, M. Ksourib, and G. Favier, "Equalization with decision delay estimation using recurrent neural networks," *Advances in Engineering Software*, vol. 36, pp. 442-447, 2005.
- [23] S. Haykin, "Adaptive digital communication receivers," *IEEE Communications Magazine*, vol. 38, pp. 106- 114, 2002.
- [24] L. Hanzo, C. H. Wong, and M. S. Yee, "Neural networked based equalization," in *Adaptive wireless transceivers*: Wiley-IEEE Press, 2002, pp. 299-383.

- [25] S. Haykin, "Neural networks expand SP's horizons," *IEEE Signal Processing Magazine*, vol. 13, pp. 24-49, 1996.
- [26] A. Hussain, J. J. Soraghan, and T. S. Durrani, "A new adaptive functional-link neural-network-based DFE for overcoming co-channel interference," *IEEE Transactions on Communications*, vol. 45, pp. 1358-1362, 1997.
- [27] C. Ching-Haur, S. Sammy, and W. Che-Ho, "A polynomial-perceptron based decision feedback equalizer with a robust learning algorithm," *Signal Processing*, vol. 47, pp. 145 - 158 1995.
- [28] B. Lu and B. L. Evans, "Channel equalization by feedforward neural networks," *IEEE International Symposium on Circuits and Systems*, vol. 5, pp. 587 - 590 1999.
- [29] B. Lu, "Wireline channel estimation and equalization." PhD Thesis, The University of Texas at Austin, 2000.
- [30] M. Ibnkahla, "Applications of neural networks to digital communications: a survey," *Signal Processing*, vol. 80 pp. 1185 - 1215 2000.
- [31] Z. Ghassemlooy and A. R. Hayes, "Digital pulse interval modulation for IR communication systems-a review," *International Journal of Communication Systems*, vol. 13, pp. 519-536, 2000.
- [32] D. C. Lee and J. M. Kahn, "Coding and equalization for PPM on wireless infrared channels," *IEEE Transaction on Communication*, vol. 47, pp. 255-260, 1999.
- [33] J. G. Proakis, *Digital communications*, Third ed. New York: McGraw-Hill, Inc., 1995.
- [34] J. C. Patra and N. R. N. Pal, "A functional link artificial neural network for adaptive channel equalization," *Signal Processing*, vol. 43, pp. 81 - 195 1995.
- [35] S. Haykin, *Neural networks: A comprehensive foundation*, 2nd ed. New Jersey, USA: Prentice Hall, 1998.
- [36] F. F. Cocchi, E. D. Di Claudio, R. Parisi, and G. Orlandi, "Improved decision feedback equalizer using discriminative neural learning," *International conference on neural networks and brain proceedings*, vol. 2, pp. 623-625, 1998.
- [37] J. B. Carruthers and J. M. Kahn, "Modeling of nondirected wireless Infrared channels," *IEEE Transaction on Communication*, vol. 45, pp. 1260-1268, 1997.
- [38] M. F. Moller, "A scaled Conjugate gradient algorithm for fast supervised learning," *Neural Networks*, vol. 6, pp. 525 - 533, 1993.
- [39] S. Rajbhandari, Z. Ghassemlooy, and M. Angelova, "The performance of PPM using neural network and symbol decoding for diffused indoor optical wireless links," in *ICTON2007*, Rome, Italy, 2007, pp. 161-164.

- [40] A. M. R. Tavares, R. T. Valadas , and A. M. d. O. Duarte, "Performance of wireless infrared transmission systems considering both ambient light interference and inter-symbol interference due to multipath dispersion," *Conference on Optical Wireless Communications*, Boston, U.S.A, 1998, pp. 82-93.
- [41] A. J. C. Moreira, R. T. Valadas, and A. M. d. O. Duarte, "Performance of infrared transmission systems under ambient light interference," *IEE Proceedings - Optoelectronics*, vol. 143, pp. 339-346, 1996.
- [42] M. D. Audeh, J. M. Kahn, and J. R. Barry, "Performance of pulse-position modulation on measured non-directed indoor infrared channels," *IEEE Transaction on Communications*, vol. 44, pp. 654-659, 1996.

List of Tables and Figures

Table 1: Simulation parameters

Fig. 1: (a) A neuron and (b) a neural network with an input, an output and a hidden layer.

Fig. 2: ANN based channel equalizer structure.

Fig. 3: The block diagram of PPM system employing ANN based equalization for diffuse optical wireless links.

Fig. 4: The flowchart for simulating the BER of PPM given in the system block diagram (Fig. 2)

Fig. 5: Normalised channel impulse response of diffuse channel (a) no equalization and (b) with equalization at $D_{rms} = 5$ ns.

Fig. 6: The BER performance against the SNR for equalized (ANN based) and the unequalized 8-PPM for LOS and diffuse links at a data rate of 155 Mbps utilizing both ‘hard’ and ‘soft’ decision decoding.

Fig. 7: The SNR requirement against the normalized D_{rms} for PPM link for a data rate of 155 Mbps, a range of M and a BER of 10^{-5} for equalized ‘soft’ decision decoding and unequalized ‘soft/hard’ decision decoding.

Table 1: Simulation parameters

| Parameters | Values |
|--|-------------------------------------|
| NN number of layers | 2 |
| NN number of neurons 1 st layer | 36 |
| NN number of neurons 2 nd layer | 1 |
| NN activation function | tan-sigmoid, log-sigmoid |
| NN training algorithm | Scaled conjugate gradient algorithm |
| NN Minimum error | 1^{-30} |
| NN Minimum gradient | 1^{-30} |
| Data rate R_b | 155 Mbps |
| Bit resolution M | 2, 3, & 4 |
| Packet length | 1000 symbols of M-bit |
| NN training length | 200 symbols of M-bit |
| Channel normalised delay spread | 0 – 4 |
| Background noise current I_b | 200 μ A |
| Photodetector responsivity R | 1 A/W |

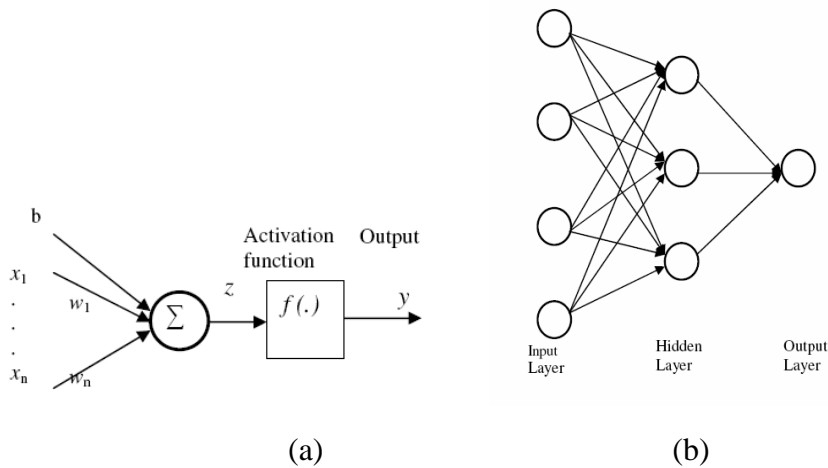


Fig. 1. (a) A neuron and (b) a neural network with an input, an output and a hidden layer.

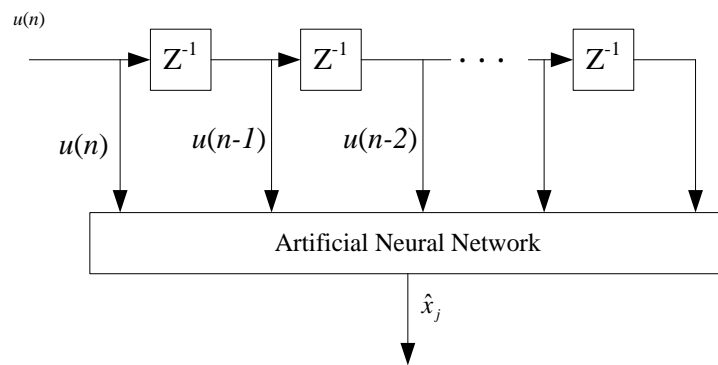


Fig. 2: ANN based channel equalizer structure.

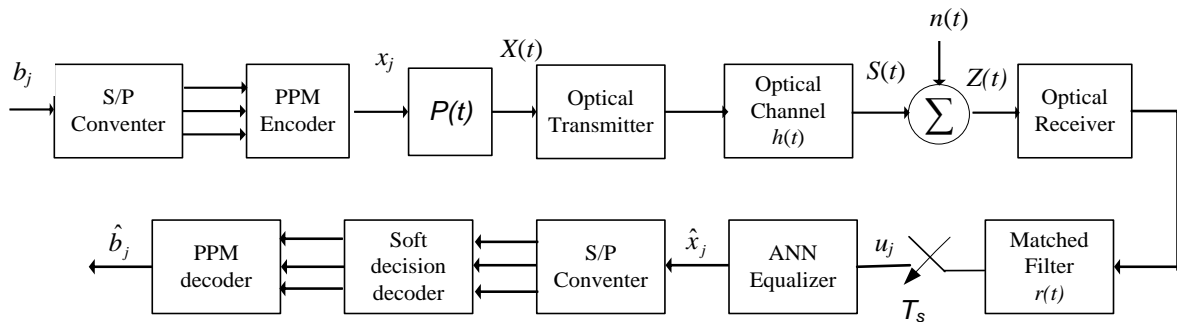


Fig. 3. The block diagram of PPM system employing ANN based equalization for diffuse optical wireless links

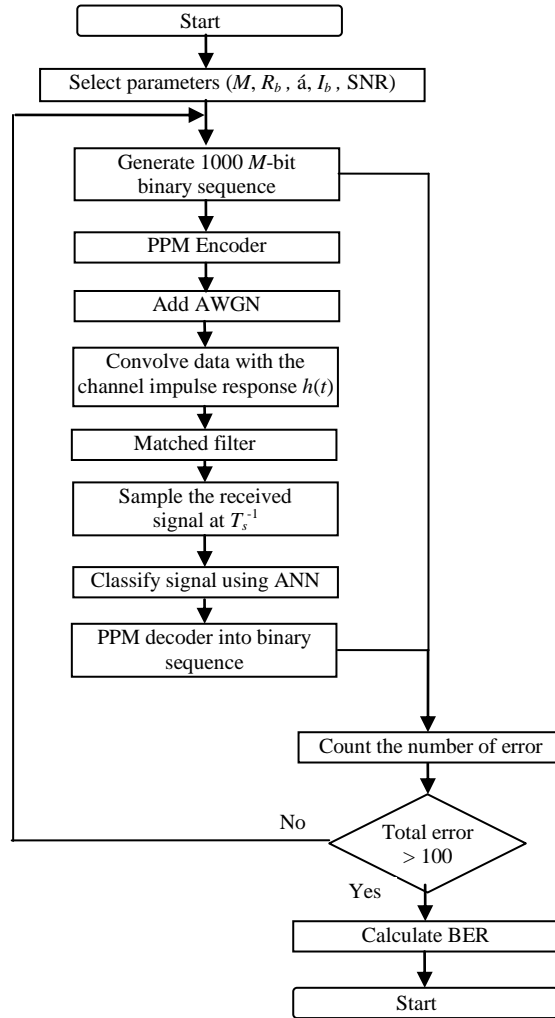
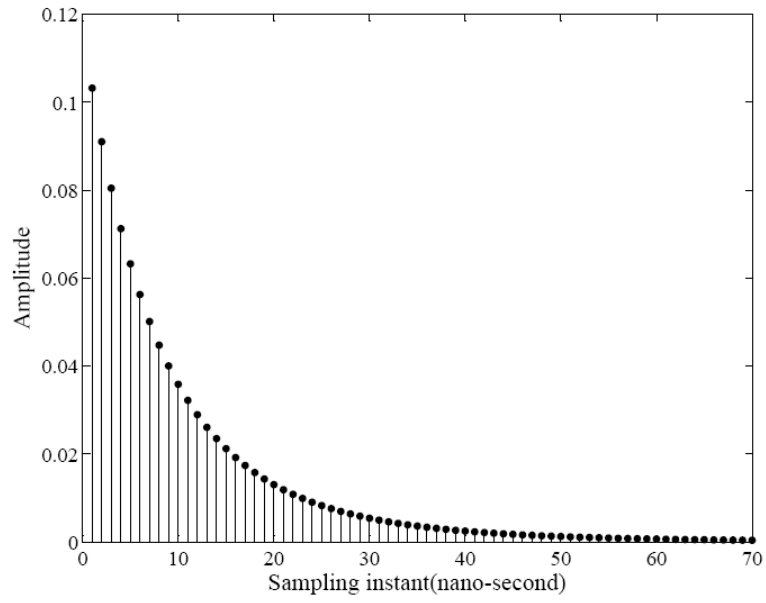
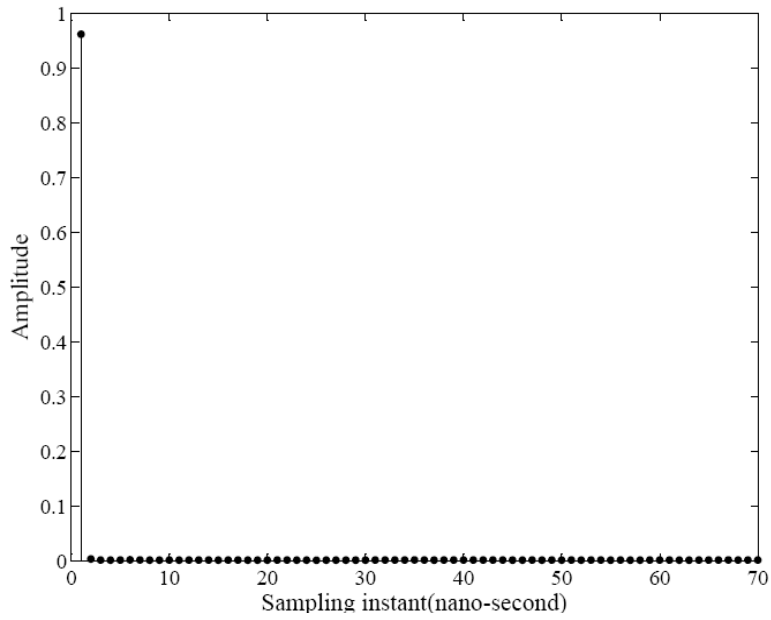


Fig. 4: The flowchart for simulating the BER of PPM given in the system block diagram (Fig. 2)



(a)



(b)

Fig. 5: Normalized channel impulse response of diffuse channel (a) no equalization and (b) with equalization at $D_{rms} = 5$ ns.

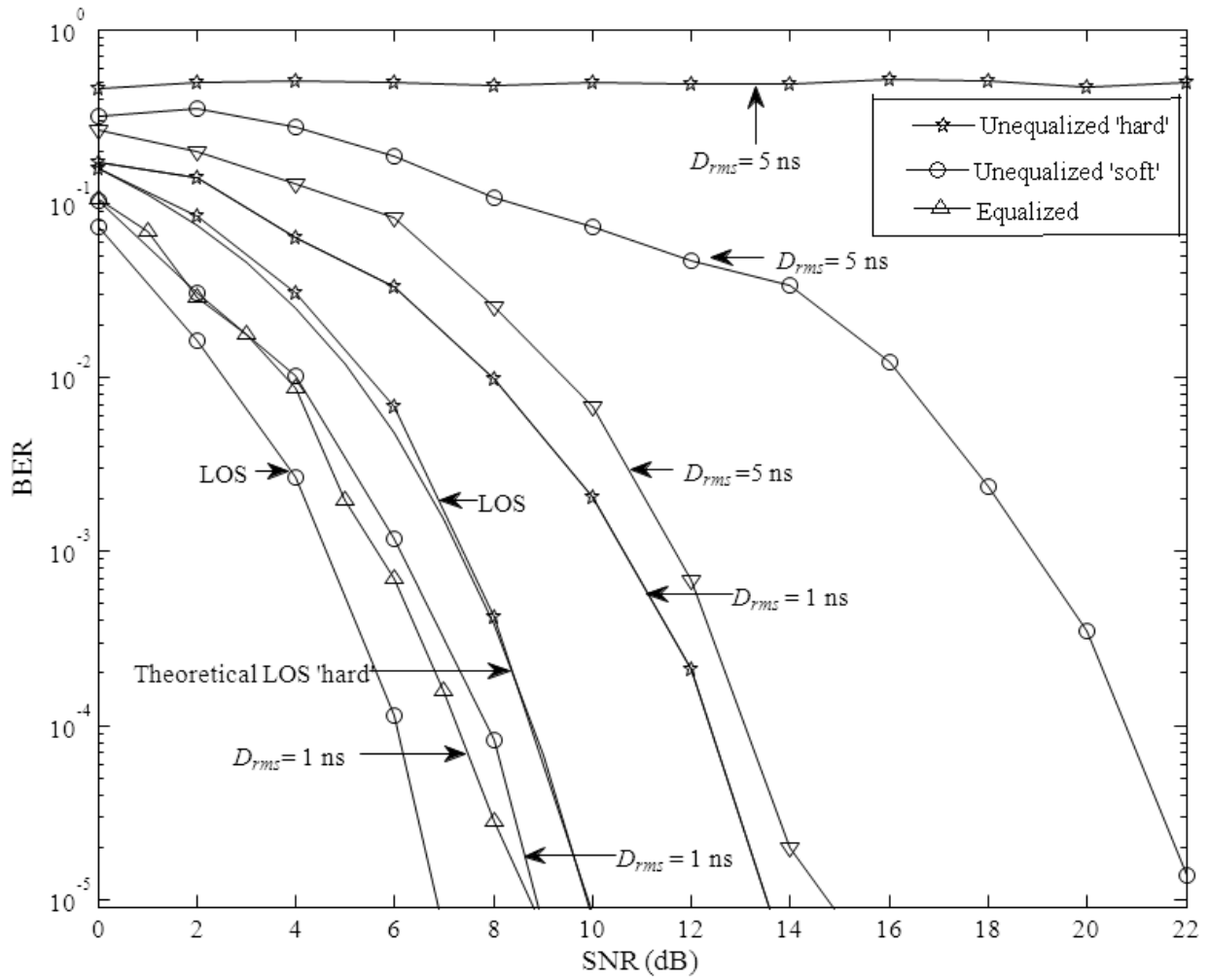


Fig. 6: The BER performance against the SNR for equalized (ANN based) and the unequalized 8-PPM for LOS and diffuse links at a data rate of 155 Mbps utilizing both 'hard' and 'soft' decision decoding.

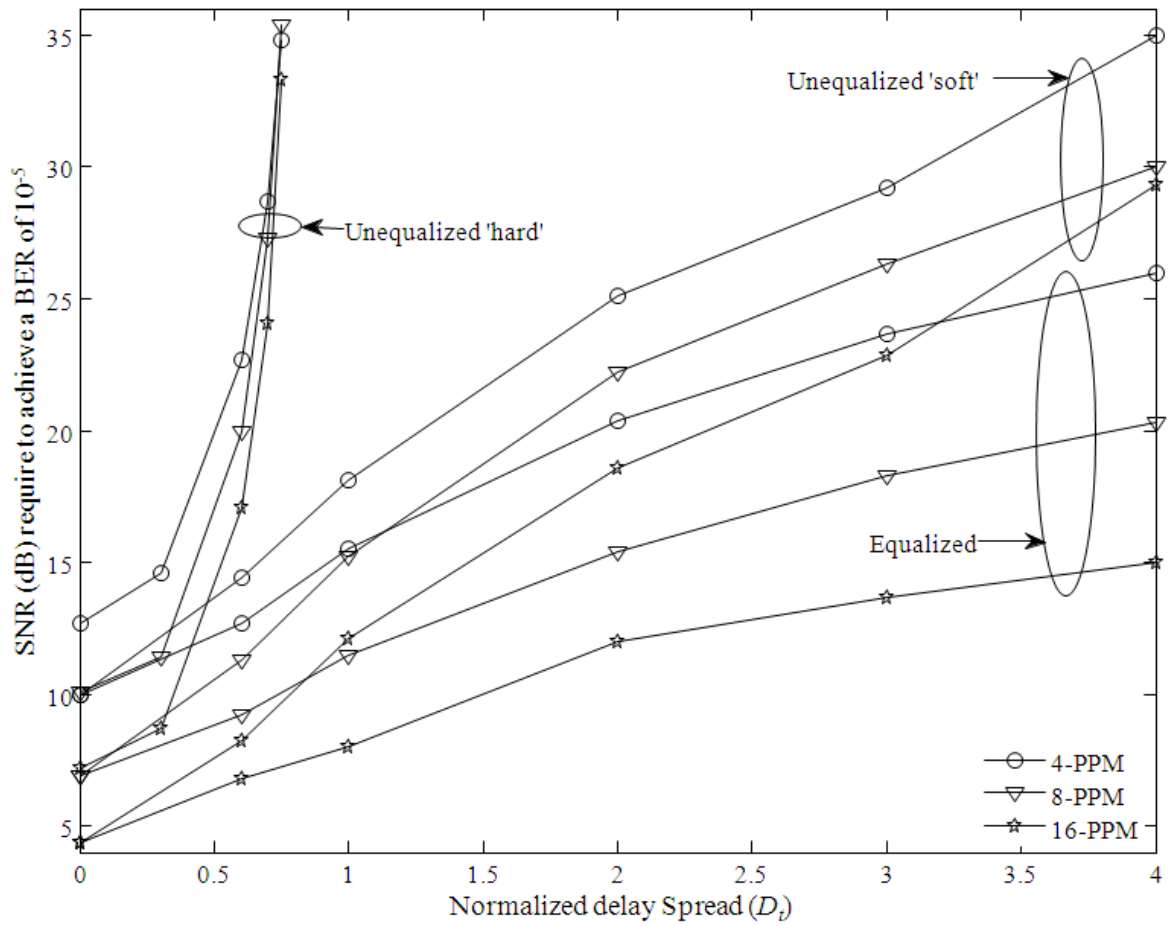


Fig. 7: The SNR requirement against the normalized D_{rms} for PPM link for a data rate of 155 Mbps, a range of M and a BER of 10^{-5} for equalized 'soft' decision decoding and unequalized 'soft/hard decision decoding.